



OPEN

Swine growth promotion with antibiotics or alternatives can increase antibiotic resistance gene mobility potential

Johanna Muurinen^{1✉}, Jacob Richert^{2,3}, Carmen L. Wickware¹, Brian Richert¹ & Timothy A. Johnson^{1✉}

Even though the use of antibiotics for food-producing animals may contribute to the emergence of antimicrobial resistance, antibiotics are still used as growth promoters. Due to consumer and regulatory pressures, the use of alternatives to antibiotics as growth promoters is increasing, thus more information is needed on their capability to disseminate antimicrobial resistance compared to antibiotics. We investigated the impacts of carbadox (antibiotic), copper sulfate and zinc oxide (metals) and mushroom powder (natural product) on the pig fecal resistome and microbiome. Antibiotic resistance gene (ARG) and mobile genetic element (MGE) abundances were measured using a high-throughput qPCR array with 382 primer pairs. Bacterial community composition was determined by 16S rRNA gene sequencing. More ARGs co-occurred with MGEs in the growth promoter group samples than in the control group samples. Community composition could not be linked to resistome in the growth promoter group samples, indicating a potential decoupling of ARGs and phylogeny. Additionally, machine-learning methods aided in defining the community and resistome differences in response to treatments. Since increased ARG mobility potential was the primary response to the dietary additives used in this study, we suggest that ARG mobility should be considered when designing antimicrobial use policies and antimicrobial resistance surveillances.

Antibiotics have been used in pork production to prevent diseases and to increase productivity since the 1940's¹. Due to the established connection of antibiotic use in animals and the emergence of antibiotic resistance in pathogenic bacteria², the regulation and prohibition of antibiotic growth promoters is increasing (prohibition in the EU in 2006¹, restrictions in 2017 in the U.S.³, and restrictions in 2020 in China⁴). Additionally, a report to the Secretary General of the United Nations suggested that antibiotic growth promoters should be completely phased out from livestock production⁵. Despite the increasing regulation, most of the world's pork is produced in countries that still allow growth promotion with antibiotics. In 2020, the U.S. was the third largest producer of pork worldwide after China and the EU, and the second largest exporter of pork meat after the EU. Currently, the livestock industries in the U.S. as well as in many other countries are looking for alternative feed additives to replace antibiotics as growth promoters due to increasing restrictions and consumer concerns towards antibiotic use in animal agriculture. Because of these reasons, the markets are now favorable to so-called alternatives to antibiotics as growth promoters and the interest towards them is increasing rapidly^{6,7}.

Among the antibiotics that are still allowed for growth promotion in the U.S., carbadox is used in pigs mainly to control dysentery and bacterial enteritis⁸. Carbadox belongs to group of chemicals known as quinoxaline 1,4-di-N-oxides, which have antibacterial effects against bacteria commonly causing diarrhea, such as *Salmonella*, *Escherichia coli* and many members of Firmicutes⁸. Carbadox can cause short-term but also long-lasting alterations in the microbiome⁹ and can promote the mobility of antibiotic resistance genes (ARGs) through transduction¹⁰. Still, little is known about the impact of carbadox or especially alternative feed additives on the abundance of ARGs in pig feces. Numerous growth promoters that are alternatives to antibiotics are currently under study for their efficacy to promote animal growth and gastrointestinal health. Among natural products, of special interest are medicinal mushrooms. *Cordyceps militaris* and *Ophiocordyceps sinensis* (formerly *C. sinensis*) produce many bioactive compounds, such as cordycepin and β -glucan, which have antimicrobial effects and

¹Department of Animal Sciences, Purdue University, West Lafayette, IN, USA. ²Department of Animal Sciences and Industry, Kansas State University, Manhattan, KS, USA. ³Present address: Department of Animal Sciences, Purdue University, West Lafayette, IN, USA. ✉email: johanna.muurinen@onehealth.fi; john2185@purdue.edu

can enhance the immune system¹¹. Zinc (Zn) and copper (Cu) are important trace elements for all organisms, and livestock animals commonly receive feed supplements that ensure their required concentration in the feed. Higher concentrations of Zn and Cu can be used for controlling various bacterial infections in livestock animals, such as diarrheal diseases⁷ and also for growth promotion^{7,12,13}. However, use of Zn oxide has shown to select zoonotic methicillin resistant *Staphylococcus aureus* (MRSA) and multiresistant *E. coli*^{14–18}. Consumption of Cu-supplemented animal feed can increase the prevalence of erythromycin resistance¹⁷ and various plasmid-mediated resistance genes in microbiomes^{17–19}. Thus, it seems that some growth promoters that are alternatives to antibiotics are actually antimicrobials and may select ARGs similarly as the antibiotics they are meant to replace.

On the other hand, when quantifying the antibiotic resistome, it is important to consider that changes in resistance gene abundance may simply be due to a change in the underlying community composition, since community composition can explain resistance gene composition^{20,21}. It is thought that growth promoters alter the gut microbial community composition, and that the microbiota composition could be manipulated to promote animal growth by inducing populations favorable to growth, immunity, and gut health²². Therefore, it is important to characterize the bacterial community composition to determine if the populations linked to induced animal growth carry ARGs and mobile genetic elements (MGEs). However, making connections between taxonomic data and resistance gene data can be challenging, since microbiome datasets are compositional and rarely meet assumptions of normality that many statistical tests require^{23,24}. In addition, it has been pointed out that different normalization strategies could influence the results derived from sequence data^{25,26}.

In order to examine the influence of carbadox, cordyceps mushroom powder and pharmacological concentrations of Zn and Cu on the community composition and resistome²⁷, we took fecal samples from pigs that were administered these growth promoters, extracted DNA, analyzed 16S rRNA gene sequences and quantified genes related to resistance and horizontal gene transfer with 382 primer pairs using a high-throughput qPCR array^{28,29}. We also compared two normalization strategies for taxonomic data using statistical analyses that are suitable for compositional datasets. Our results suggest that inclusion of ARGs into MGEs led to decoupling of bacterial community composition and resistome composition in response to growth promotion, highlighting the importance of MGEs in shaping the resistomes under the influence of different types of antimicrobial agents.

Results

Samples and data quality control. Samples were collected from pigs that had been assigned into non-treatment control group (NTC = no antibiotic or alternative growth promoters), or one of the growth promoter groups (AB = carbadox, M = mushroom powder mixture of *C. militaris* and *O. sinensis*, ZnCu = Zn oxide and Cu sulfate). Each treatment group consisted of six pens and each pen had seven pigs. To capture a representative microbiota of the pens that would show the influence of treatments instead of differences between individual pigs, the DNA for 16S rRNA gene sequencing was extracted from combined fecal samples of one medium weight female and male per pen. After quality filtering, a total of 741,785 sequences were obtained. For 22 samples sequences per sample ranged from 11,392 to 67,072. Two samples were discarded due to low number of sequences, resulting in five samples in the NTC and AB groups. The data analysis for 16S rRNA gene sequencing was completed using two different methods: rarefaction and subsampling or total sum scaling (TSS). The TSS normalized 16S rRNA gene sequence data had 132 operational taxonomical units (OTUs), while rarefied and subsampled 16S rRNA gene sequence data 127 OTUs. The same DNA samples were used for qPCR array analysis to examine how the treatments altered the resistome. One hundred and thirty-six assays out of 382 assays (Supplementary Table S1) targeting antibiotic resistance genes (ARGs) or mobile genetic elements (MGEs) were positive. See materials and methods for qPCR data processing and Ct value adjustment for four assays that had unspecific amplification.

The profiles of most abundant genera and genes were similar in different treatment groups.

To take into account the influence of normalization of 16S rRNA gene sequence reads on the results, we used two different normalization methods. Only small differences were discovered between TSS normalized and rarefied and subsampled OTUs among the most abundant genera (Fig. 1A,B). The TSS normalized OTUs and rarefied and subsampled OTUs correlated significantly ($\rho = 0.97$, $p < 0.05$) (Supplementary Fig. S1), indicating the agreement of the overall community composition of the two normalization methods. *Prevotella* was the most abundant genera in all treatments and all samples had several short chain fatty acid producers (Fig. 1A,B). Genera belonging to Gammaproteobacteria, which also contains many well-known pathogens, were not among the most abundant OTUs (Fig. 1A,B). Very few OTUs were found only in one treatment group with both normalization methods and a majority of the OTUs were found in all treatment groups, however more OTUs were found in all treatment groups using TSS normalization than rarefied and subsampled normalization (Fig. 1D,E).

The different treatment groups also had similar resistome profiles (Fig. 1C). The NTC group had the highest number of positive assays (110), the AB group had 106 positive assays, The M group had 100 positive assays and the ZnCu group had 103 positive assays. Twenty-eight genes were detected in only one treatment group, but most genes were found in all treatment groups (Fig. 1F). Out of the positive assays, 108 targeted ARGs and 28 MGEs. Among the detected ARGs, 63 conferred resistance to aminoglycosides, MLSBs or tetracyclines and the most common resistance mechanism was antibiotic deactivation (Supplementary Fig. S2A,B). Among MGEs, most of the positive assays targeted insertion sequences (12) or transposases (7) (Supplementary Fig. S2C).

Growth promoters favored different genera, ARGs and MGEs. Generalized linear models (GLMs) with False discovery rate control³⁰ for p -value adjustment were used for testing which genera, ARGs and MGEs differed in abundance between treatments. Mostly only minor differences in abundance of different genera were found between treatment groups (Supplementary Fig. S3A,B). Compared to all other growth promoters, carba-

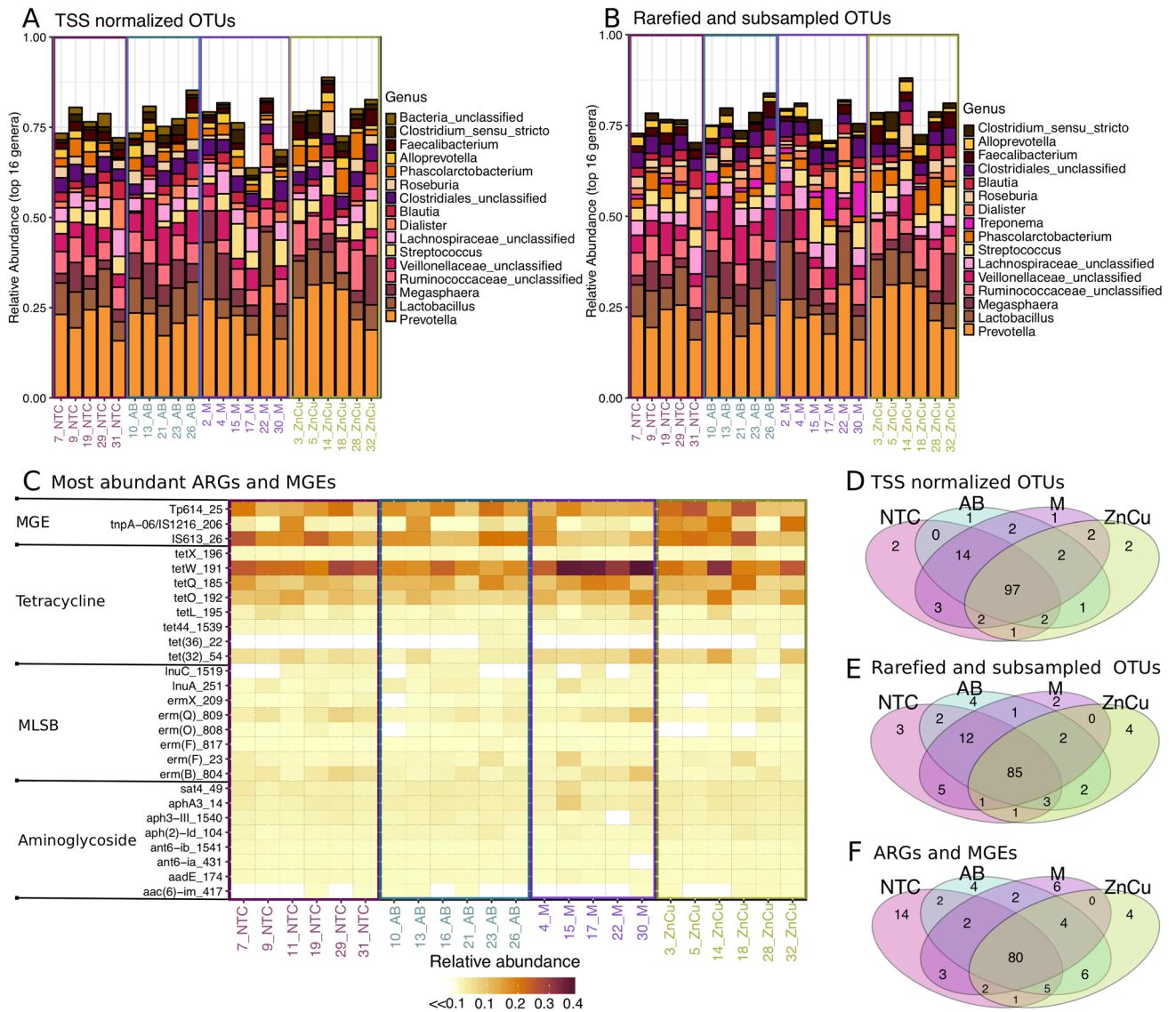


Figure 1. Comparison of the most abundant genera, ARGs and MGEs in different treatment groups. Samples on x-axis are grouped according to the treatments and color-coded. Sample names are as follows: *NTC* non-treatment control, *AB* carbadox (antibiotic), *M* mushroom powder, *ZnCu* zinc oxide and copper sulfate. The number in front of the group code denotes the number of the pen. (A) Stacked bar plot showing 16 most abundant genera in OTUs normalized using total sum scaling (TSS). (B) Stacked bar plot showing 16 most abundant genera in rarefied and subsampled OTUs. (C) Most abundant genes related to antibiotic resistance and mobile genetic elements (n = 27). Each row represents results of each primer set (assay) (Supplementary Table S1) displayed on the y-axis. Assays are grouped according to the antibiotic group which the target genes confer resistance. MLSB is abbreviation for Macrolide – Lincosamide – Streptogramin B resistance and MGE for mobile genetic elements. One sample from mushroom powder group was left out from the qPCR array analysis due to a technical error. (D) Venn diagram showing the OTUs that are shared between samples belonging into different treatment groups when TSS normalization was used. (E) Venn diagram showing the OTUs that are shared between samples belonging into different treatment groups when Rarefying and subsampling was used. (F) Venn diagram showing the ARGs and MGEs that are shared between samples belonging into different treatment groups.

dox favored unclassified *Veillonellaceae* in feces and decreased the abundance of *Streptococcus*, whereas Zn and Cu decreased the abundance of *Bifidobacterium* and *Campylobacter* (adjusted *p*-value < 0.05, gamma distribution GLMs [TSS OTUs] and negative binomial GLMs [rarefied and subsampled OTUs]) (Fig. 2A,B, Supplementary Tables S2 and S3). Mushroom powder decreased the abundance of fecal *Roseburia* and favored *Campylobacter* compared to other treatments (adjusted *p*-value < 0.05, gamma distribution GLMs [TSS OTUs] and negative binomial GLMs [rarefied and subsampled OTUs]) (Fig. 2A,B, Supplementary Tables S2 and S3). *Streptococcus* was more abundant in M and ZnCu group samples compared to other groups (adjusted *p*-value < 0.05, gamma distribution GLMs [TSS OTUs] and negative binomial GLMs [rarefied and subsampled OTUs]) (Fig. 2A,B, Supplementary Tables S2 and S3). More ARGs and MGEs were differentially abundant in NTC group and M group

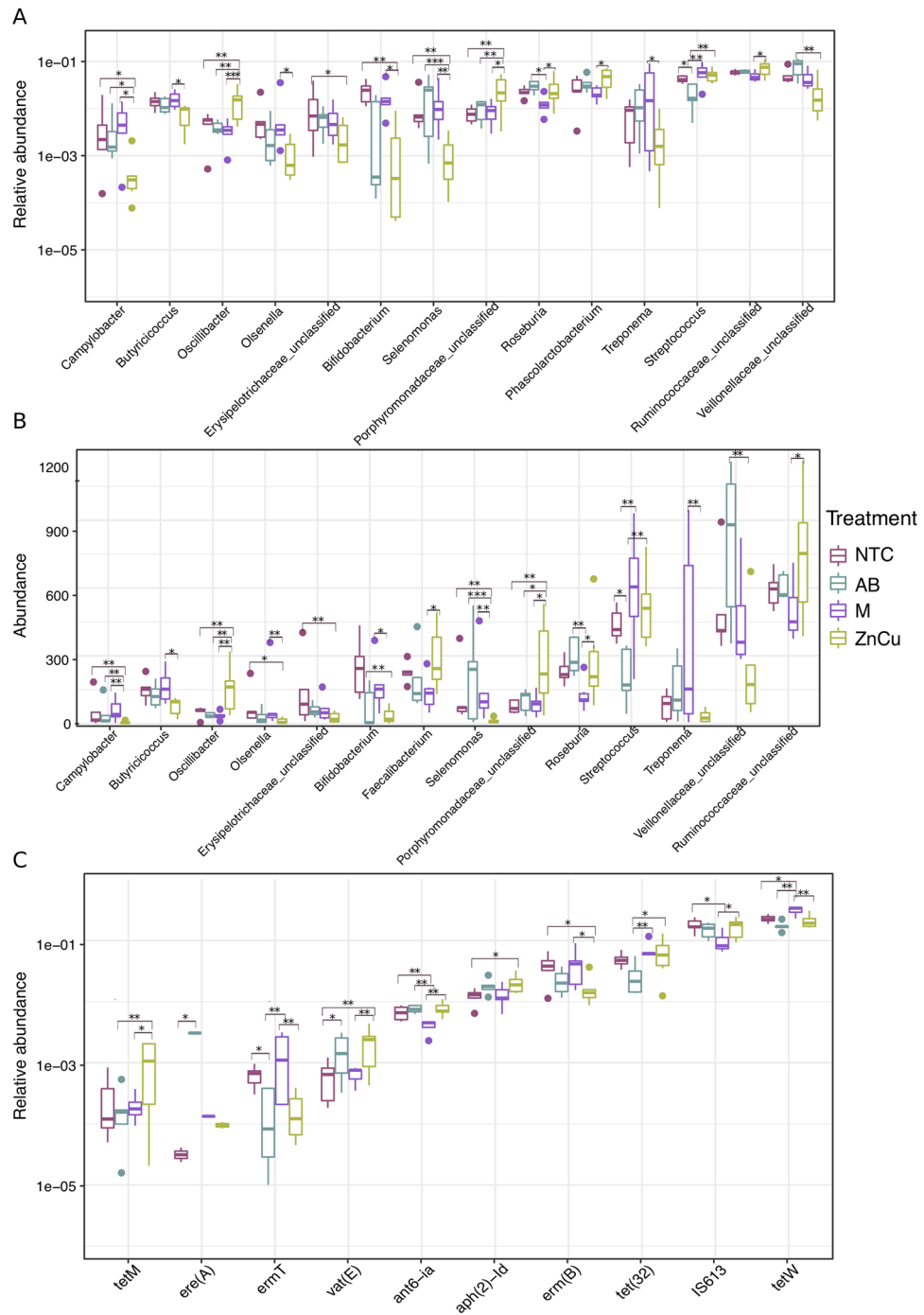


Figure 2. Boxplots showing the most abundant genera, ARGs and MGEs with statistically significant differences between treatment groups labeled on right. *NTC* non-treatment control, *AB* carbadox (antibiotic), *M* mushroom powder, *ZnCu* zinc oxide and copper sulfate. The asterisks “*”, “**” and “***” denote statistical significance levels at $p < 0.05$, $p < 0.01$ and $p < 0.001$, respectively. **(A)** Most abundant genera in TSS normalized OTUs ($n = 14$), **(B)** most abundant genera in rarefied and subsampled OTUs ($n = 14$), **(C)** most abundant genes related to resistance and transfer ($n = 10$). See Supplementary Fig. S3A, B and C for all differentially abundant genera and ARGs and MGEs and Supplementary Tables S2, S3 and S4 for fold changes of the differently abundant genera and ARGs and MGEs.

comparison than when NTC group was compared to ZnCu or AB groups (Supplementary Fig. S3C). Compared to all other growth promoters, carbadox and Zn and Cu increased the relative abundance of *vat(E)*, mushroom powder increased the relative abundance of *tetW*, and Zn and Cu favored *tetM* (adjusted p -value < 0.05 , gamma

distribution GLMs) (Fig. 2C, Supplementary Table S4). Interestingly, carbadox treatment decreased the relative abundance of *tetW*, *tet(32)*, *erm(B)*, *ermT* and *tetM* compared to other treatments or to NTC group (adjusted p -value < 0.05 , gamma distribution GLMs) (Fig. 2C, Supplementary Table S4).

Both OTU normalization methods yielded similar results for differential OTU abundance in the treatment groups (Fig. 2A,B). The exceptions were that *Phascolarctobacterium* was among the differentially abundant genera when TSS normalization was used, whereas *Faecalibacterium* was differentially abundant when rarefying and subsampling was used (Fig. 2A,B) and that more genera were differentially abundant when TSS normalization was used (Supplementary Tables S2 and S3).

Growth promoters had modest influences on overall bacterial community composition and resistome. With both TSS normalized OTUs and rarefied and subsampled OTUs, the treatment group explained 24% of the variability in community composition (PERMANOVA, $R^2 = 0.239$, $p < 0.05$). With ARGs and MGEs, the treatment group explained 27% of the variability (PERMANOVA, $R^2 = 0.267$, $p < 0.05$). The number of sequences per sample was also included as a variable in the PERMANOVA model with both normalization methods, but the library size did not have influence on the community variability in our samples ($p > 0.05$).

The different growth promoters altered the community composition and resistome only slightly, since in all non-metric multidimensional scaling (NMDS) ordinations the samples belonging to different treatment groups clustered close to each other with mostly overlapping centroid confidence intervals (Fig. 3A,B,D). In ordinations of TSS normalized and rarefied and subsampled OTU-tables, the ZnCu group tended to cluster further away from the other samples indicating more dissimilar community composition (Fig. 3A,B), however there were no significant differences between treatment groups among pairwise PERMANOVA comparisons (False discovery rate control adjusted³⁰ p -value > 0.05). In the ordination of the ARG and MGE data, there was no separation between ZnCu group and the other groups, instead the M group clustered slightly separately (Fig. 3D) and in the pairwise comparisons using the ARG and MGE data, M vs. AB group explained 32% of the variance (PERMANOVA, $R^2 = 0.321$, False discovery rate control adjusted²⁹ p -value < 0.05), but in all the other pairwise comparisons the differences were nonsignificant (False discovery rate control adjusted³⁰ p -value > 0.05).

Taxonomic variation did not explain resistome variation in growth promoter group samples. The OTU ordinations were correlated against each other and against the ARG and MGE NMDS ordination using Procrustes analysis to determine if the taxonomic variation explains resistome variation. The two OTU NMDS ordinations had reasonably high (0.7) and significant ($p < 0.05$) correlation and the Procrustes residual error remained lower than 0.25 in all samples except one (Fig. 3C). The correlation between the rarefied and subsampled OTU ordination (which did not include all the data due to subsampling) and the ARG and MGE ordination was moderately high (0.6, $p < 0.05$) and there was no pattern in Procrustes residual errors across different samples (Fig. 3F). Contrariwise, the correlation between the TSS normalized OTU ordination (that included all quality filtered data) and the ARG and MGE ordination was nonsignificant ($p > 0.05$) and Procrustes residual errors were high in most samples not belonging to NTC group, in which the residual errors were mostly equal or less than the first quantile residual value (Fig. 3E). The Procrustes analyses performed on TSS normalized OTUs and resistome implies that taxonomic variation explained resistance variation in NTC samples with less error. However, growth promoters altered the resistome, resulting in higher residual errors in samples belonging to AB, M and ZnCu groups and thus the overall correlation between TSS normalized OTU ordination and ARG and MGE ordination was not significant (Procrustes analysis, $p > 0.05$).

The links between bacterial community structure and resistome were further examined with Mantel's test using Spearman's rank correlation. The correlation coefficients between the TSS normalized OTUs and ARGs and MGEs distance matrices as well as the rarefied and subsampled OTUs and ARGs and MGEs distance matrices were low ($\rho = 0.25$ and $\rho = 0.23$, respectively, $p < 0.05$), which suggests that the phylogenetic composition did not govern the resistome composition when all samples were included in the analysis. We also used Mantel's test for all treatment groups individually. With the NTC group and both OTU normalization methods, the bacterial community distance matrix correlated significantly with the distance matrix obtained from ARGs and MGEs ($\rho = 0.66$ [TSS OTUs] and $\rho = 0.62$ [rarefied and subsampled OTUs], $p < 0.05$). With all growth promoter groups and both OTU normalization methods, the correlations between OTU and ARG and MGE distance matrices were nonsignificant, giving more evidence that the growth promoters shaped the resistance composition and thus taxonomic variation did not explain the resistance variation in the growth promoter group samples. It should be denoted that we had only five or six samples in each treatment group; however, the results were consistent, since the correlations between taxonomic structure and resistome were reasonably high and significant in NTC group and nonsignificant in all other groups.

Growth promoters increased the co-occurrences of ARGs and MGEs. A correlation matrix between ARG and MGE relative abundances was visualized using network analysis to examine if the growth promoters selected resistance genes into mobile genetic elements. The network of NTC group was simpler compared to growth promoter group networks as the number of correlating ARGs and MGEs increased in response to growth promotion (Fig. 4). There were no integrons co-occurring with resistance genes in the NTC group network, but integrons were present in all the growth promoter group networks (Fig. 4) and co-occurred with many ARGs. A gene that is essential to the conjugative transfer system of F plasmids, *trb-C³¹*, was present in the network of M and ZnCu groups, correlating with several ARGs (Fig. 4). AB and M group networks had more aminoglycoside resistance genes than other networks and M group also had the most multidrug resistance genes, but the least tetracycline resistance genes, whereas AB group network had the most vancomycin resistance genes (Fig. 4).

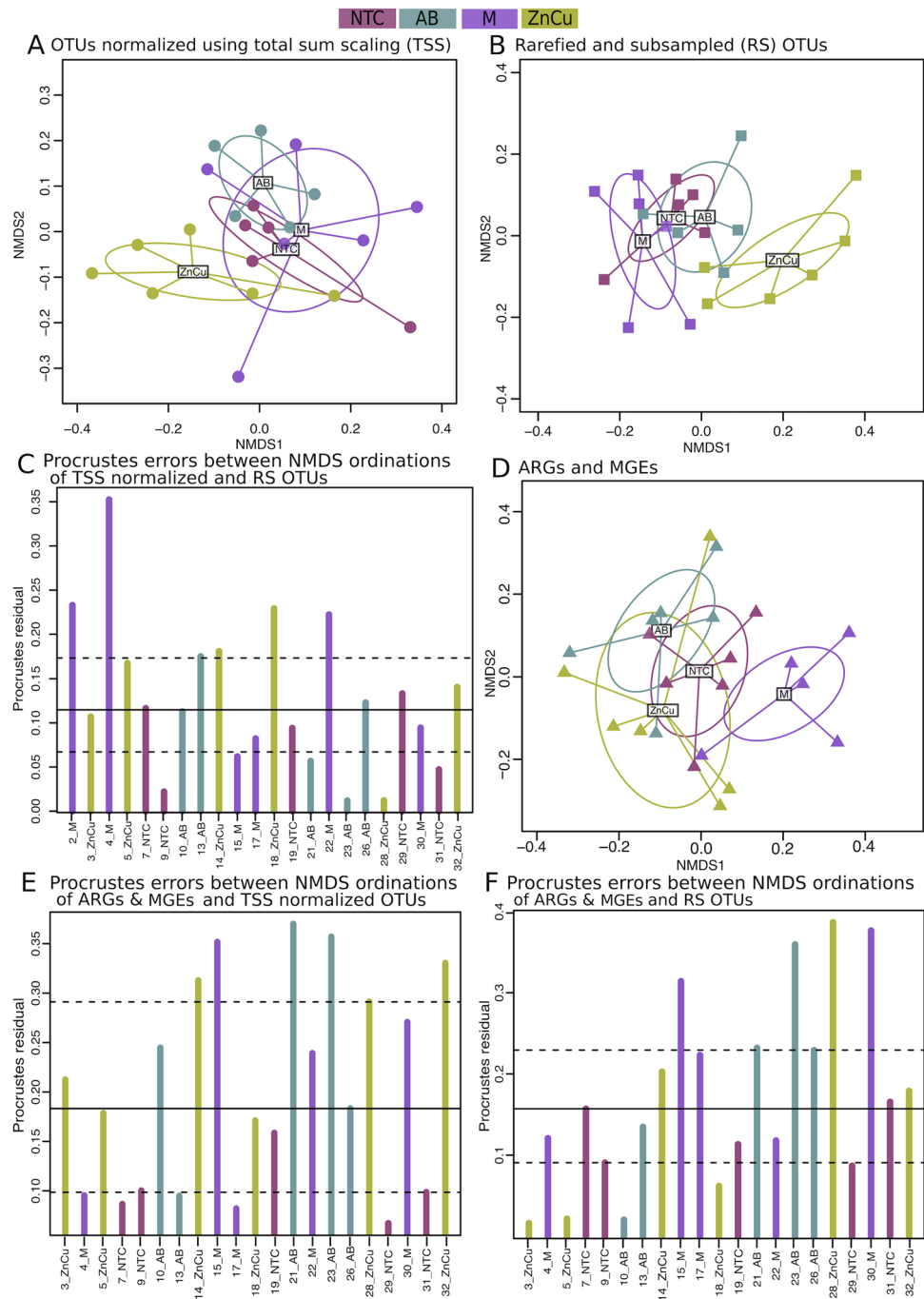


Figure 3. NMDS ordinations of TSS normalized OTUs, rarefied and subsampled OTUs and ARGs and MGEs and procrustes errors between them. Sample names are as follows: *NTC* non-treatment control, *AB* carbadox (antibiotic), *M* mushroom powder, *ZnCu* zinc oxide and copper sulfate. The number in the sample name denotes the number of the pen. **(A)** NMDS ordination of TSS normalized OTUs. **(B)** NMDS ordination of rarefied and subsampled (RS) OTUs. **(C)** Procrustes errors between NMDS ordinations of TSS normalized OTUs and rarefied and subsampled OTUs. **(D)** NMDS ordination of ARGs and MGEs. **(E)** Procrustes errors between NMDS ordinations of TSS normalized OTUs and ARGs and MGEs. **(F)** Procrustes errors between NMDS ordinations of rarefied and subsampled OTUs and ARGs and MGEs. The Procrustes residual error line plots (**C**, **E**, **F**) allow residual error size comparisons. The bars show the difference in the community structures between the two normalization methods (**C**) as well as the differences in community structure and resistome structure in samples belonging to different treatment groups (**E**,**F**). Horizontal lines denote the median (solid), 25% and 75% quantiles (dashed).

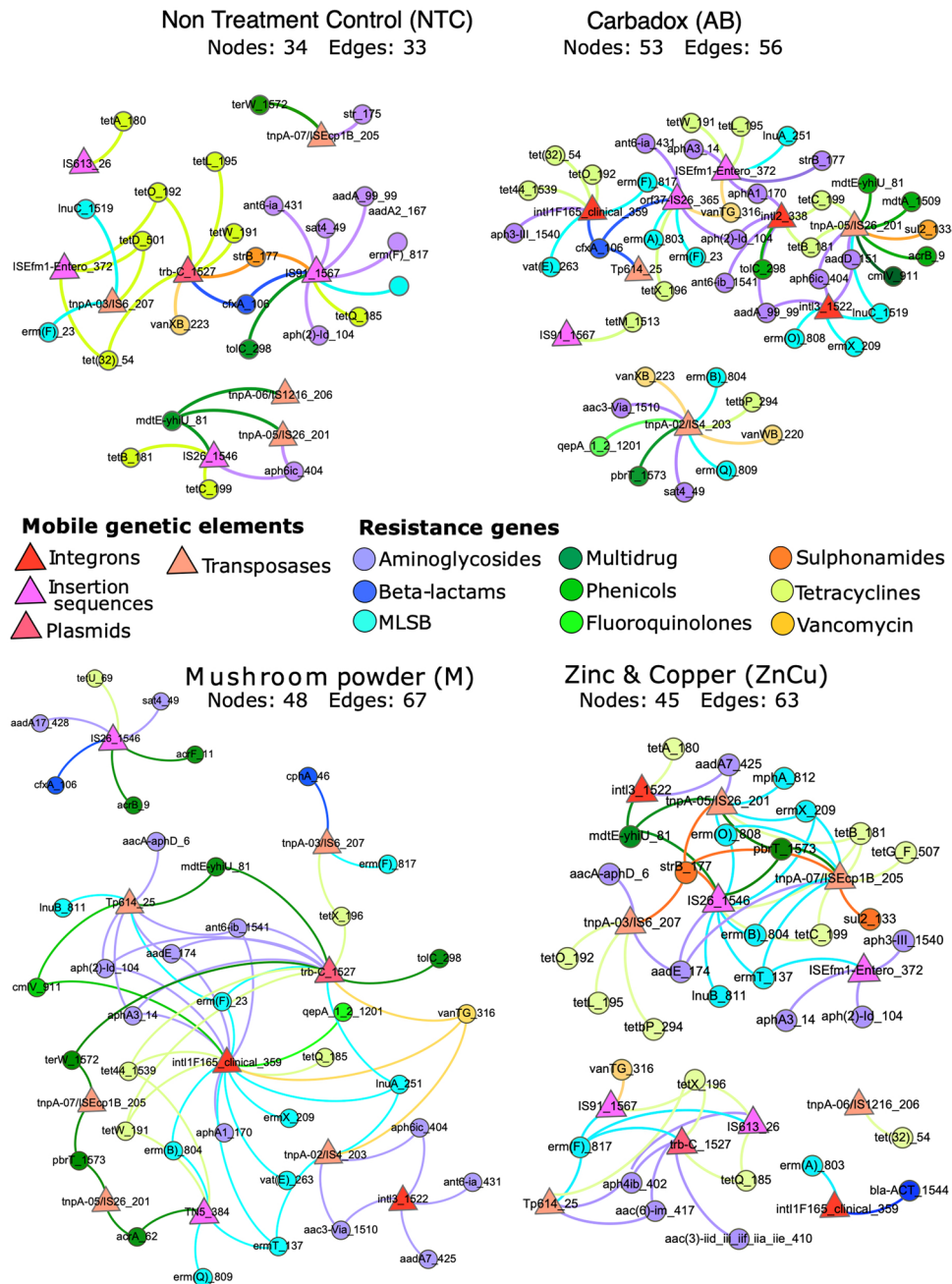


Figure 4. Network analysis showing co-occurrence patterns between ARGs and MGEs within the samples in different treatment groups. Nodes of the MGEs are triangles, and circle resistance gene nodes are colored according to the antibiotic they confer resistance. Edges between resistance gene nodes and mobile genetic element nodes have the color of the resistance gene node. Nodes have equal sizes, edges have equal weights, and distance between the nodes is irrelevant. Numbers of nodes and edges were higher in the growth promoter groups (AB, M and ZnCu) than in the control group network (NTC), suggesting increased ARG mobility potential in response to growth promotion.

Transposase gene for insertion sequence-like element IS1216 was the best predictor for resistance and community composition. We used machine-learning approaches to identify drivers of changes in community composition. First, a cluster analysis was performed on a combined data table of TSS normalized OTUs and ARGs and MGEs using *t*-distributed stochastic neighbor embedding (t-SNE) algorithm³² and HDBSCAN algorithm³³. Then, a classification random forests model^{33,34} was used for identifying the predictors for the clustering pattern. Three clusters were identified after dimension reduction. Most of the samples belonged to cluster 2, while cluster 1 had two ZnCu samples, one M group sample and one AB group sample, and cluster 3 contained only three ZnCu samples (Fig. 5A). According to the partial dependence plot that shows the most

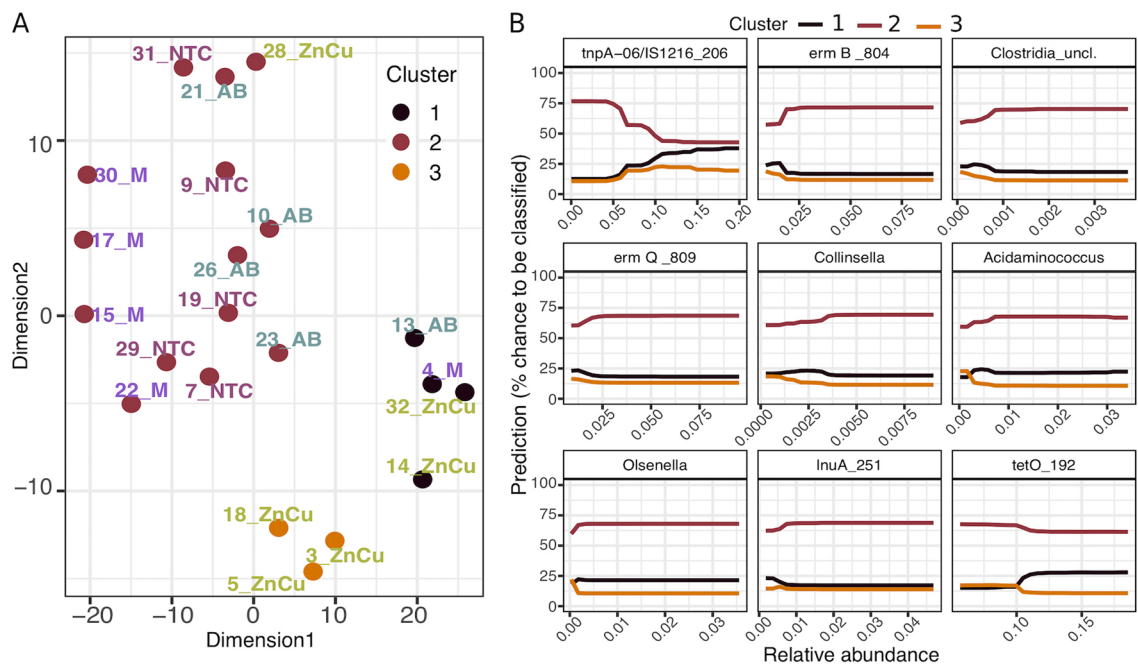


Figure 5. t-SNE analysis of a dataset containing ARGs, MGEs and TSS normalized OTUs (all relative abundances). **(A)** The clustering pattern of the samples. **(B)** Partial dependence plot of cluster numbers and the most important predictors in the order of decreasing importance. The partial dependence plot shows the effect of each predictor on the model outcome one by one, while the other predictors are fixed to their average value.

important predictors found by the classification random forests model, clusters 1 and 3 were separated from cluster 2 due to higher abundance of transposase gene linked to *IS1216* element and from each other because the abundance of *tetO* was lower in cluster 3 (Fig. 5B). Five of the nine best predictors for clustering pattern were MGEs and ARGs and four were bacterial genera (Fig. 5B). Interestingly, only one of the ZnCu group samples belonged to cluster 2, while all the other ZnCu samples clustered to clusters 1 and 3. Thus, growth promotion with Zn and Cu might cause more alterations in the community composition and resistome than the other growth promoters examined in this study.

Discussion

Our study explored the influences of antibiotic and alternative growth promoters on the pig fecal resistome, ARG mobility, and bacterial community composition. Resistome structure and taxonomic structure were correlated in the NTC group samples, but there was no correlation between resistome and phylogeny in the growth promotion groups. Some have reported that community composition predicts resistance profile^{19,20,36}, while others have reported that under the presence of a selective pressure, phylogeny and resistome can become uncoupled in the swine feces and manure³⁷. Our network analysis revealed that the growth promoters in this study increased linkages between ARGs and MGEs, i.e. more ARGs correlated with MGEs in the resistome of growth promoter group pigs than in the resistome of NTC group pigs. Thus, it seems plausible that resistance gene mobility would have increased in response to growth promotion, since subinhibitory antimicrobial concentrations and bacterial stress response mechanisms can induce horizontal gene transfer^{38–40}.

However, only one gene linked to plasmid conjugation was found in our networks (*trb-C* in the networks of M and ZnCu groups) and most plasmid-associated sequences our primers targeted were not detected. Nevertheless, the genes associated to insertion sequences in transposons, which had increased linkages to ARGs in our networks, are commonly embedded in plasmids^{41–43}. The primers targeting plasmids were either validated against a mock community consisting of 28 sequenced strains carrying plasmids, or originated from earlier studies, in which plasmids were typically searched from certain sample types, such as soils²⁹. Sequences of plasmids belonging into the same incompatibility group can have variation depending on species or even strains carrying the plasmids^{44,45} and therefore it is possible that the transposons in our networks were embedded in plasmids even though the plasmids could not be detected.

Under the influence of bactericidal substances, the integrase genes can be upregulated as well as cell competence induced, and both of these mechanisms have been shown to promote horizontal acquisition of ARGs^{40,46}. The increased connections between integrons and ARGs in our networks would support the theory that ARGs were incorporated into MGEs due to enhanced cell competence and integration under the influence of growth promoters. Besides the inclusion of ARGs into MGEs, another possible scenario is that bacteria carrying MGEs with multiple ARGs and other embedded features would have tolerated the growth promoters better than bacteria carrying MGEs with only few ARGs, possibly due to more variability in stress response mechanisms^{17,37,38}. Despite the mechanism, more ARGs co-occurring with MGEs in response to growth promotion could indicate

more persistent resistance gene collection³⁸ and potential for ARGs to be mobilized by the MGEs in the future, and this way the ARGs in the animal microbiomes could eventually be transmitted to human microbiomes^{2,38}.

Notwithstanding the changes in ARG mobility potential, the abundances of nearly all ARGs and MGEs were on similar levels in the non-treatment control group and the growth promoter groups, which indicates that it is unlikely that changing the substance that is used for growth promotion would reduce antimicrobial resistance in the pig fecal microbiome, at least in a short period of time (33 days in this study). Gut bacteria, especially gram-negative species, are known to carry many ARGs and MGEs and the gastro-intestinal tract is suspected to be a major hotspot for horizontal gene transfer^{38,48}. These observations have also been made with individuals without antibiotic exposure^{49,50}.

Interestingly, some ARGs were less abundant in the AB group than in the NTC group and alternative growth promoter groups. A potential explanation for this could be that carbadox is a broad acting antibiotic and suppresses most bacterial populations^{8,9}. Overall, we did not observe large shifts among genera as a result of growth promotion feed additives. Bifidobacteria, which have been previously linked to lower antibiotic resistance level^{51,52}, were somewhat more abundant in the NTC and M group samples; however, in this study the ARG abundances in samples belonging to different groups were similar. It is possible that the shifts in the community composition caused by growth promoters were small with high between-pen variability and thus the changes in the community structure are difficult to capture with community-wide molecular approaches. We hypothesize that the effects of broad-spectrum antibiotics and alternatives are difficult to capture because the response will be varied, depending on the initial bacterial community to which they are applied. Efforts to standardize the initial microbial community may allow more reproducible effects between replicates. In this study, while we did not observe strong changes in specific genes, it was the greater context of the genes that was altered indicating an increased gene mobility potential.

Although the changes in community composition and resistome in response to treatments were modest and mostly nonsignificant, we observed shifts with machine learning methods. The differences we observed did not precisely follow the experimental grouping (but largely isolated the ZnCu group), and therefore they were not found with commonly used ordination methods or differential abundance analysis. The transposase gene linked to IS1216 element was the driver for the clustering result and has been previously associated to Gram-positive bacteria^{37,53}, such as *Enterococcus faecium*⁵⁴. However, *Enterococcus* or other known Gram-positive carriers of IS1216 were not among the predictors of the clustering result in random forest analysis. Even though we cannot demonstrate all the factors explaining the clustering result, the observation that zinc and copper treatment perhaps altered the microbiome and resistome more than the other treatments would not have been possible without the use of a machine learning approach for statistical analyses. Thus, machine learning is an important tool in determining the complex relationship between resistome and bacterial community compositions.

Considering the two approaches to normalize OTU counts between samples, the rarefied and subsampled OTU data and TSS normalized OTU data mostly agreed; however, in Procrustes analysis, the rarefied and subsampled OTU data correlated significantly with the resistome data when all samples were used, although the same analysis using the TSS normalized data as input showed that the taxonomic data did not explain resistance. It is important to acknowledge that rarefying and subsampling captures the most abundant OTUs for each sample²⁶ and discards rare OTUs, as well as slightly adjusting OTU relative abundances in different samples. If the sample size and differences in OTU abundances are small before the procedure, the shifts might change the outcome if rarefied OTU data is used in comparison with data obtained using a different method. Thus, researchers making connections between taxonomic data and resistome observations should use multiple methods to confirm their findings.

In this experiment, we observed that growth promoting feed additives increased co-occurrences between ARGs and MGEs, which could have caused the decoupling of phylogeny and resistance gene composition also observed in response to growth promotion. These observations indicate that the studied feed-additives can increase and maintain resistance gene mobility potential. On the other hand, under this experimental design, the withdrawal of antibiotics did not decrease the abundance of antibiotic resistance, however, we did not detect enrichment of ARGs in response to growth promotion either. Thus, we suggest that the mobility potential of ARGs should be considered to be included in antimicrobial resistance surveillances to establish the impact of changes in agricultural practices on antimicrobial resistance.

Materials and methods

Animal experiment statement. All procedures involving animal use were approved by the Purdue University Animal Care and Use Committee (protocol #1303000841). Animal care and use standards were based upon the Guide for the Care and Use of Agricultural Animals in Research and Teaching⁵⁵ and were performed in accordance with guidelines and regulations of National Institutes of Health's Office of Laboratory Animal Welfare. Study design, animal experiment and reporting followed the ARRIVE guidelines (<https://arriveguidelines.org/arrive-guidelines>).

Samples and DNA. The pig fecal samples were obtained from growth promoter experiment⁵⁶ where 210 weanling pigs ((Duroc × (York × Landrace)) avg. 19 d of age and 5.8 kg were used in a 33-day trial. The experiment had 7 pigs in each pen and 6 pens per each treatment. Feed amendment treatments were: (1) non-treatment control (NTC); (2) antibiotic growth promoter (carbadox, 55 ppm) (AB); (3) mushroom powder (mixture of *C. militaris* and *O. sinensis*, 300 ppm) (M); (4) carbadox and mushroom powder mixture (results are not included in this study); (5) copper sulfate (125 ppm) and zinc oxide (3000 ppm d 0–7, 2000 ppm d 7–35) (ZnCu). The animal experiment is described in more detail in⁵⁶. After 33 days, fecal samples were taken from 1 median weight female and male per pen. Samples from the same pen were pooled, and DNA was extracted using the

DNeasyPowerLyzer PowerSoil DNA Isolation Kit (Qiagen) according to the manufacturer's protocol. Extracted DNA was stored at -20°C before 16S sequencing and qPCR array.

16S sequencing and quantitative PCR array. The 16S rRNA gene library was constructed as described⁵⁷. Briefly, the V4 region of the bacterial 16S rRNA gene was amplified with 515R (GTGCCAGCMGCCGCGGTAA)/806R (GGACTACHVGGGTWTCTAAT) primers. 16S rRNA gene libraries were also prepared for a known mock community (20 Strain Even Mix Genomic Material; ATCC MSA-1002TM) and a no-template control (water). The amplified DNA from one 96-well plate was normalized using a SequalPrep Normalization Plate (Invitrogen), and pooled into a single library. Library concentrations were determined using the KAPA Library Quantification Kit (Roche) and the average fragment length was determined using a high sensitivity kit with the Bioanalyzer (Agilent). The pooled samples, mock community, and water were sequenced with Illumina MiSeq v2 (500 cycles). Sequences were demultiplexed using oligonucleotide barcode sequences and Illumina software.

Quantitative PCR reactions and raw data processing were conducted using WaferGen SmartChip Real-time PCR system as reported⁵⁸. The qPCR array reactions were performed using 384 previously described and validated primer sets (assays) (Supplementary Table S1)²⁹. One sample from M group (2_M) was not included in the qPCR array analysis due to technical error. Samples from pigs that received both mushroom powder and carbadox were also excluded and therefore the results from 16S rRNA amplicon sequencing are not presented in this study.

16S sequence analysis and qPCR array data processing. The 16S rRNA amplicon sequences were analyzed using mothur (v 1.39.3)⁵⁷: contigs were made from paired forward and reverse raw reads, aligned to reference sequences (SILVA database release 132)⁵⁹, screened and filtered to remove low quality reads (ambiguous bases allowed=0, maximum read length=275, homopolymers allowed=8), classified with reference to known taxonomic classifications (RDP training set 16)⁶⁰ and clustered into OTUs. The sequences clustered into 137 different OTUs at the 3% dissimilarity level. One NTC group sample (11_NTC) and one AB group sample (16_AB) were discarded due to low number of obtained sequences. 16S sequences were normalized using two different methods: total sum scaling (TSS) using R and rarefying and subsampling using mothur. To produce the rarefied and subsampled OTU table, the data were subsampled to 7500 reads per sample according to rarefaction curves (Supplementary Fig. S4). The rarefied and subsampled OTU table and only quality filtered OTU table (for TSS) were imported into R. After removing the results of samples from animals that received both mushroom powder and carbadox, 132 different OTUs remained in the TSS normalized OTU table and 127 different OTUs in the rarefied and subsampled OTU table. The TSS normalization was carried out in R by dividing each OTU read count by the total number of reads in that sample and all the NA observations (zero sequences) were replaced with $1.490935\text{e}-07$, which was 100-fold lower than the lowest observed relative abundance.

In the qPCR array, assays “16S old 1_1”, “blaOXY-1_1118”, “cmlV_911”, “czcA_1536”, “fabK_1520”, “int11F165_clinical_359” and “tetPA_1507” were positive in the negative control, however the Ct-values in the negative control were mostly higher than in experimental samples (Supplementary Table S5). Assay “tetPA_1507” was detected only in the negative control and the Ct-values of assay “czcA_1536” were removed from the results since they were lower in the negative control than in samples. Assay “16S old 1_1” results were removed and not used in normalization since DNA amplification was more efficient in assay “16S new 2_2”. The Ct-values of the remaining four assays that were positive in the negative control were adjusted as follows: the Ct values of each of these assays in each sample were subtracted from Ct value of the assay in the negative control. The resulting numbers were then subtracted from 27, which was the Ct value was used as the cutoff between true positive values and primer-dimer amplification. Next, all the Ct values that were higher than 27 were set to “NA”. After this, all the assays that were undetected in all the samples were removed, resulting in 136 assays out of 382 targeting to AGRs or MGEs being included in the data table. The ΔCt values, $\Delta\Delta\text{Ct}$ values and relative gene abundances were calculated from these Ct values as previously described²⁸. Genes under the detection limit were given a ΔCt value of 20, which was higher than any observed ΔCt (17.4).

Statistical analyses. R version 3.5.1 (2018-07-02) was used for data exploration, graphics and for all statistical analyses. Analysis of differential abundances of taxa and ARGs and MGEs were carried out using gamma distribution GLMs with TSS normalized OTUs and ARGs and MGEs (relative abundances) and negative binomial GLMs with rarefied and subsampled OTUs (abundance). Gamma distribution model was selected because the relative abundance values (TSS normalized OTUs and ARGs and MGEs) did not fit to normal distribution but followed the gamma distribution. Negative binomial models were selected for rarefied and subsampled OTUs because of the overdispersion in the abundance data. With both model types, *p*-values were obtained with Tukey's post-hoc test and adjusted with False discovery rate control³¹ using *glht* function in the multcomp package⁶¹.

The community and resistome compositions were analyzed using vegan package⁶². PERMANOVA was used to examine the shifts in community composition and resistome between treatment groups with function *adonis* and 9999 permutations. Nonmetric multidimensional scalings (NMDS) were completed using the Bray–Curtis dissimilarity index with function *metaMDS*. Procrustes analysis with the *protest* function was used to examine the agreement of ordinations of TSS normalized OTUs and rarefied and subsampled OTUs as well as ordination of ARGs and MGEs and both OTU ordinations separately. Mantel's test and Spearman's rank correlation was used to analyze the links between microbial community structure and resistome: first, Bray–Curtis dissimilarity indexes were calculated for TSS normalized OTUs, rarefied and subsampled OTUs and for ARGs and MGEs with function *vegdist*. Then the *mantel* function was applied for the dissimilarity indexes of TSS normalized OTUs

and ARGs and MGEs as well as rarefied and subsampled OTUs and ARGs and MGEs. Mantel's tests between both OTU dissimilarity matrices and dissimilarity matrix of ARGs and MGEs were also run for all the treatment groups separately.

To examine if the treatments selected resistance genes into mobile genetic elements, a correlation matrix between ARG and MGE relative abundances was visualized using network analysis with Gephi⁶³ (Fig. 4). Spearman's rank correlations between ARGs and MGEs within treatment groups and their *p*-values used in network analysis were obtained with package psych⁶⁴ using False discovery rate control³¹. Only ARG-MGE-pairs that were detected at least in three samples with a strong positive correlation ($\rho > 0.8$, adjusted *p*-value < 0.05) were included.

The factors influencing the shifts in taxonomic structure and resistome were analyzed with machine learning algorithms as previously described⁶⁵. First, dimension reduction was executed on a combined data table of TSS normalized OTUs and ARGs and MGEs using t-SNE algorithm³² and the R package Rtsne⁶⁶, with 50,000 iterations and "perplexity" set to 5. Then, clusters in the two-dimensional data were identified using HDBSCAN algorithm³³ in the package dbscan⁶⁷. The minimum number of members in clusters ("minPts") was set to 3. Classification random forest model³⁴ was used with partial dependence plot function in edarf package⁶⁸ for identifying the most important predictors for the clustering pattern. The forests were grown to 10,000 trees using the ranger package⁶⁹ and the best predictors were screened using Gini index by adding predictors one at a time in the order of decreasing importance⁷⁰. The final model was then selected according to the highest Cohen's Kappa (comparison of observed accuracy and expected accuracy).

Data availability

Raw reads from 16S rRNA gene amplicon sequencing are deposited under BioProject accession number PRJNA605462 at NCBI. The R code, mothur commands and all datasets used in statistical analyses are available at <https://github.com/sjmuurine/ZnCu>.

Received: 13 October 2020; Accepted: 8 January 2021

Published online: 09 March 2021

References

- Dibner, J. J. & Richards, J. D. Antibiotic growth promoters in agriculture: history and mode of action. *Poult. Sci.* **84**, 634–643 (2005).
- Marshall, B. M. & Levy, S. B. Food animals and antimicrobials: Impacts on human health. *Clin. Microbiol. Rev.* **24**, 718–733 (2011).
- Centner, T. J. Recent government regulations in the United States seek to ensure the effectiveness of antibiotics by limiting their agricultural use. *Environ. Int.* **94**, 1–7 (2016).
- Hu, Y. J. & Cowling, B. J. Reducing antibiotic use in livestock, China. *Bull. World Health Organ.* **98**, 360–361 (2020).
- Interagency Coordination Group on Antimicrobial Resistance (IACG). No time to wait: securing the future from drug-resistant infections. (2019).
- Thacker, P. A. Alternatives to antibiotics as growth promoters for use in swine production: A review. *J. Anim. Sci. Biotechnol.* **4**, 35–35 (2013).
- Willing, B. P. *et al.* Bacterial resistance to antibiotic alternatives: A wolf in sheep's clothing?. *Anim. Front.* **8**, 39–47 (2018).
- Cheng, G. *et al.* Quinoxaline 1,4-di-N-oxides: Biological activities and mechanisms of actions. *Front. Pharmacol.* **7**, 64 (2016).
- Looft, T., Allen, H. K., Casey, T. A., Alt, D. P. & Stanton, T. B. Carbadox has both temporary and lasting effects on the swine gut microbiota. *Front. Microbiol.* **5**, 1–1 (2014).
- Johnson, T. A. *et al.* The in-feed antibiotic carbadox induces phage gene transcription in the swine gut microbiome. *mBio* **8**, e00709–17 (2017).
- Richert, J. *et al.* Effects of cordyceps mushroom powder on nursery pig performance. *Kansas Agric. Exp. Station Res. Rep.* **4**, (2018).
- Di Giancamillo, A. *et al.* Copper sulphate forms in piglet diets: Microbiota, intestinal morphology and enteric nervous system glial cells. *Anim. Sci. J.* **89**, 616–624 (2018).
- Jacela, J. Y., DeRouchey, J. M., & Tokach, M. D., *et al.* Feed additives for swine: Fact sheets – high dietary levels of copper and zinc for young pigs, and phytase.
- Slifierz, M. J., Friendship, R. & Weese, J. S. Zinc oxide therapy increases prevalence and persistence of methicillin-resistant staphylococcus aureus in pigs: A randomized controlled trial. *Zoonoses Public Health* **62**, 301–308 (2015).
- Bednorz, C. *et al.* The broader context of antibiotic resistance: Zinc feed supplementation of piglets increases the proportion of multi-resistant Escherichia coli in vivo. *Int. J. Med. Microbiol. IJMM* **303**, 396–403 (2013).
- Ciesinski, L. *et al.* High dietary zinc feeding promotes persistence of multi-resistant E. coli in the swine gut. *PLoS ONE* **13**, 1–18 (2018).
- Poole, K. At the nexus of antibiotics and metals: The impact of Cu and Zn on antibiotic activity and resistance. *Trends Microbiol.* **25**, 820–832 (2017).
- Yazdankhah, S., Rudi, K. & Bernhoft, A. Zinc and copper in animal feed - development of resistance and co-resistance to antimicrobial agents in bacteria of animal origin. *Microbial Ecol. Health Dis.* <https://doi.org/10.3402/mehd.v25.25862> (2014).
- Fang, L. *et al.* Co-spread of metal and antibiotic resistance within ST3-IncHI2 plasmids from E. coli isolates of food-producing animals. *Sci. Rep.* **6**, 25312 (2016).
- Munk, P. *et al.* Abundance and diversity of the faecal resistome in slaughter pigs and broilers in nine European countries. *Nat. Microbiol.* **3**, 898–908 (2018).
- Forsberg, K. J. *et al.* Bacterial phylogeny structures soil resistomes across habitats. *Nature* **509**, 612–616 (2014).
- Ward, T. L. *et al.* Antibiotics and host-tailored probiotics similarly modulate effects on the developing avian microbiome, mycobiome, and host gene expression. *mBio* **10**, e02171–19 (2019).
- Gloor, G. B., Macklaim, J. M., Pawlowsky-Glahn, V. & Egozcue, J. J. Microbiome datasets are compositional: And this is not optional. *Front. Microbiol.* **8**, 2224 (2017).
- Zuur, A. F., Ieno, E. N. & Elphick, C. S. A protocol for data exploration to avoid common statistical problems. *Methods Ecol. Evol.* **1**, 3–14 (2010).
- McMurdie, P. J. & Holmes, S. Waste Not, Want Not: Why Rarefying Microbiome Data Is Inadmissible. *PLoS Computat. Biol.* **10**, (2014).
- Weiss, S. *et al.* Normalization and microbial differential abundance strategies depend upon data characteristics. *Microbiome* **5**, 27–27 (2017).
- Wright, G. D. The antibiotic resistome: the nexus of chemical and genetic diversity. *Nat. Rev. Microbiol.* **5**, 175–186 (2007).

28. Muurinen, J., Karkman, A. & Virta, M. High Throughput Method for Analyzing Antibiotic Resistance Genes in Wastewater Treatment Plants. In *Antimicrobial Resistance in Wastewater Treatment Processes* 253–262. (John Wiley & Sons, Inc., 2017).
29. Stedtfield, R. D. *et al.* Primer set 2.0 for highly parallel qPCR array targeting antibiotic resistance genes and mobile genetic elements. *FEMS Microbiol. Ecol.* **94**, (2018).
30. Benjamini, Y. & Hochberg, Y. Controlling the false discovery rate: A practical and powerful approach to multiple testing. *J. Roy. Stat. Soc.: Ser. B (Methodol.)* **57**, 289–300 (1995).
31. Maneewannakul, S., Maneewannakul, K. & Ippen-Ihler, K. Characterization of trbC, a new F plasmid tra operon gene that is essential to conjugative transfer. *J. Bacteriol.* **173**, 3872–3878 (1991).
32. Van Der Maaten, L. Accelerating t-SNE using tree-based algorithms. *J. Mach. Learn. Res.* **15**, 3221–3245 (2014).
33. Campello, R. J. G. B., Moulavi, D. & Sander, J. Density-Based Clustering Based on Hierarchical Density Estimates. in *Advances in Knowledge Discovery and Data Mining* (eds. Pei, J., Tseng, V. S., Cao, L., Motoda, H. & Xu, G.) 160–172 (Springer Berlin Heidelberg, 2013).
34. Breiman, L. Random forests. *Mach. Learn.* **45**, 5–32 (2001).
35. Liaw, A. & Wiener, M. Classification and regression by randomForest. *R news* **2**, 18–22 (2002).
36. Su, J. Q. *et al.* Antibiotic resistome and its association with bacterial communities during sewage sludge composting. *Environ. Sci. Technol.* **49**, 7356–7363 (2015).
37. Johnson, T. A. *et al.* Clusters of antibiotic resistance genes enriched together stay Together in Swine Agriculture. *mBio* **7**, e02214–15 (2016).
38. Davies, J. & Davies, D. Origins and evolution of antibiotic resistance. *Microbiol. Mol. Biol. Rev.* **74**, 417–433 (2010).
39. Poole, K. Bacterial stress responses as determinants of antimicrobial resistance. *J. Antimicrob. Chemother.* **67**, 2069–2089 (2012).
40. Wellington, E. M. H. *et al.* The role of the natural environment in the emergence of antibiotic resistance in gram-negative bacteria. *Lancet Infect. Dis.* **13**, 155–165 (2013).
41. Sivertsen, A. *et al.* The enterococcus cassette chromosome, a genomic variation enabler in enterococci. *mSphere* **3**, e00402–18 (2018).
42. Harmer, C. J., & Hall, R. M. IS26-mediated formation of transposons carrying antibiotic resistance genes. *mSphere* **1**, e00038–16 (2016).
43. Garcillán-Barcia, M. P. & de la Cruz, F. Distribution of IS91 family insertion sequences in bacterial genomes: Evolutionary implications. *FEMS Microbiol. Ecol.* **42**, 303–313 (2002).
44. Phan, M.-D. *et al.* Variation in *Salmonella enterica* Serovar Typhi IncHI1 plasmids during the global spread of resistant typhoid fever. *Antimicrob. Agents Chemother.* **53**, 716 (2009).
45. Zrimec, J. & Lapanje, A. DNA structure at the plasmid origin-of-transfer indicates its potential transfer range. *Sci. Rep.* **8**, 1820 (2018).
46. Prudhomme, M., Attaiech, L., Sanchez, G., Martin, B. & Claverys, J.-P. Antibiotic stress induces genetic transformability in the human pathogen *Streptococcus pneumoniae*. *Science* **313**, 89 (2006).
47. Enne, V. I. *et al.* Assessment of the fitness impacts on *Escherichia coli* of acquisition of antibiotic resistance genes encoded by different types of genetic element. *J. Antimicrob. Chemother.* **56**, 544–551 (2005).
48. Netherwood, T. *et al.* Gene transfer in the gastrointestinal tract. *Appl. Environ. Microbiol.* **65**, 5139–5141 (1999).
49. Moore, A. M. *et al.* Gut resistome development in healthy twin pairs in the first year of life. *Microbiome* **3**, 27 (2015).
50. Gibson, M. K. *et al.* Developmental dynamics of the preterm infant gut microbiota and antibiotic resistome. *Nat. Microbiol.* **1**, 16024 (2016).
51. Pärnänen, K. *et al.* Maternal gut and breast milk microbiota affect infant gut antibiotic resistome and mobile genetic elements. *Nat. Commun.* **9**, 3891 (2018).
52. Taft, D. H. *et al.* Bifidobacterial dominance of the gut in early life and acquisition of antimicrobial resistance. *mSphere* **3**, e00441–18 (2018).
53. Partridge, S. R., Kwong, S. M., Firth, N. & Jensen, S. O. Mobile genetic elements associated with antimicrobial resistance. *Clin. Microbiol. Rev.* **31**, e00088–117 (2018).
54. Clewell, D. B. *et al.* Extrachromosomal and mobile elements in enterococci: transmission, maintenance, and epidemiology. in *Enterococci: From commensals to leading causes of drug resistant infection [Internet]* (Massachusetts Eye and Ear Infirmary, 2014).
55. Chapter 11: Swine in *Guide for the Care and Use of Agricultural Animals in Research and Teaching*. 143–155 (Federation of Animal Science Societies 2010).
56. Richert, J. *et al.* Evaluating the interactive effects of cordyceps mushroom powder and carbadox to pharmacological copper and zinc for nursery pigs. *Kansas Agric. Exp. Station Res. Rep.* **5**, (2019).
57. Kozich, J. J., Westcott, S. L., Baxter, N. T., Highlander, S. K. & Schloss, P. D. Development of a dual-index sequencing strategy and curation pipeline for analyzing amplicon sequence data on the MiSeq illumina sequencing platform. *Appl. Environ. Microbiol.* **79**, 5112 (2013).
58. Wang, F. *et al.* High throughput profiling of antibiotic resistance genes in urban park soils with reclaimed water irrigation. *Environ. Sci. Technol.* **48**, 9079–85 (2014).
59. Quast, C. *et al.* The SILVA ribosomal RNA gene database project: improved data processing and web-based tools. *Nucleic Acids Res* **41**, D590–D596 (2013).
60. Cole, J. R. *et al.* Ribosomal database project: Data and tools for high throughput rRNA analysis. *Nucleic Acids Res.* **42**, D633–D642 (2013).
61. Hothorn T. *et al.* Package ‘multcomp’. Simultaneous inference in general parametric models. <https://CRAN.R-project.org/package=multcomp> (2016).
62. Oksanen, J. *et al.* vegan: Community Ecology Package. <https://CRAN.R-project.org/package=vegan> (2019).
63. Bastian M., Heymann S. & Jacomy M. Gephi: an open source software for exploring and manipulating networks. *International AAAI Conference on Weblogs and Social Media*. <http://www.aaai.org/ocs/index.php/ICWSM/09/paper/view/154> (2009).
64. Revelle, W. psych: Procedures for Personality and Psychological Research. <https://CRAN.R-project.org/package=psych> (2019).
65. Ruuskanen, M. O. & St Pierre, K. A. Physicochemical drivers of microbial community structure in sediments of Lake Hazen, Nunavut, Canada. *Front Microbiol* **9**, 1138 (2018).
66. Krijthe J. & van der Maaten L. Rtsne: T-distributed stochastic neighbor embedding using a Barnes-hut implementation. <https://cran.r-project.org/web/packages/Rtsne/index.html> (2018).
67. Hahsler M., Piekenbrock M., Arya S. & Mount D. dbscan: Fast Density-Based Clustering with R. *J. Stat. Softw.* **91**, 1–30. <https://CRAN.R-project.org/package=dbscan> (2019).
68. Jones Z. & Linder F. edarf: Exploratory data analysis using random forests. *J. Open Source Softw.* **1**:92. <https://CRAN.R-project.org/package=edarf> (2017).
69. Wright M. N. & Ziegler A. ranger: A fast implementation of random forests for high dimensional data in C++ and R. *J. Stat. Softw.* **77**, 1–17. <https://CRAN.R-project.org/package=ranger> (2017).
70. Menze, B. H. *et al.* A comparison of random forest and its Gini importance with standard chemometric methods for the feature selection and classification of spectral data. *BMC Bioinf.* **10**, 213–213 (2009).

Acknowledgements

We thank Ms. Olivia Consoli for excellent technical assistance in laboratory analysis and Purdue University for internal financial support. Information Technology at Purdue is acknowledged for providing computational resources.

Author contributions

J.M. and C.W. analyzed the data (bioinformatics and statistical analyses) and J.M. wrote the main manuscript text. J.R. was responsible for the practical implementation of the pig feeding trial and fecal sampling. B.R., J.R. and T.A.J. designed the animal experiment and sampling. T.A.J. and C.W. supervised the laboratory work. All authors contributed to manuscript revisions and have read and approved the final version of the manuscript.

Competing interests

The authors declare no competing interests.

Additional information

Supplementary Information The online version contains supplementary material available at <https://doi.org/10.1038/s41598-021-84759-9>.

Correspondence and requests for materials should be addressed to J.M. or T.A.J.

Reprints and permissions information is available at www.nature.com/reprints.

Publisher's note Springer Nature remains neutral with regard to jurisdictional claims in published maps and institutional affiliations.



Open Access This article is licensed under a Creative Commons Attribution 4.0 International License, which permits use, sharing, adaptation, distribution and reproduction in any medium or format, as long as you give appropriate credit to the original author(s) and the source, provide a link to the Creative Commons licence, and indicate if changes were made. The images or other third party material in this article are included in the article's Creative Commons licence, unless indicated otherwise in a credit line to the material. If material is not included in the article's Creative Commons licence and your intended use is not permitted by statutory regulation or exceeds the permitted use, you will need to obtain permission directly from the copyright holder. To view a copy of this licence, visit <http://creativecommons.org/licenses/by/4.0/>.

© The Author(s) 2021